
M.E. KORNIENKO, N.L. SHEIKO, O.M. KORNIENKO, T.YU. NIKOLAIENKO

Taras Shevchenko National University of Kyiv, Faculty of Physics
(64, Volodymyrs'ka Str., Kyiv 01601, Ukraine; e-mail: nikkorn@univ.kiev.ua)

**DISCRETE PROPERTIES OF QUASILIQUID
WATER FILM IN THE ICE PREMELTING RANGE.
1. TEMPERATURE DEPENDENCES OF WATER
NANOFILM THICKNESS AND VISCOELASTIC
PROPERTIES OF POLYCRYSTALLINE ICE**

PACS 68.18.Fg, 62.25.-g

Peculiarities in the temperature dependences of the properties of quasiliquid water films on the surface of ice crystallites have been studied experimentally under ice premelting conditions. Viscoelastic properties of polycrystalline ice in the temperature interval from -60 to 20 °C have been analyzed. Peculiarities in the temperature dependences of the water nanolayer thickness, $L(T)$, and the imaginary part of the shear modulus (modulus of viscous losses), $G_2(T)$, are found. Quasiequidistant temperature variations of the viscous loss modulus are revealed for the first time. A comparison of the results obtained with literature data on the temperature dependences $L(T)$, the density of water in nanolayers, and the ice surface roughness allowed us to associate the observed features with a discrete cluster structure of quasiliquid water nanofilms. Temperature intervals of the enhanced stability for a cluster structure of water nanofilms are revealed, which manifest themselves in the form of extrema in viscoelastic ice parameters in the premelting interval. The interrelation between the phenomena of ice premelting and temperature discretization at the melting in ice nanolayers is considered for the first time.

Keywords: viscoelastic properties, premelting, quasiliquid

1. Introduction

Though such phenomena as the ice premelting and the existence of quasiliquid water nanofilms on the ice surface are known since Faraday's and Thompson's time, this field is actively studied till now [1–7]. In the modern scientific literature, a considerable body of experimental results has been accumulated concerning the researches of properties of quasiliquid water films on the ice surface at temperatures from -30 to 0 °C, i.e. lower than the melting temperature of massive ice. Among the recent results, the discovery of such a phenomenon as a drastic temperature decrease on the ice surface, when approaching

the melting temperature and in the course of melting, and the accompanying increase in the electric conductivity of water nanofilms and the ice antireflection in the microwave range [5, 6] should be emphasized, as well as an effective draining of quasiliquid films over the ice surface at -20 °C, which is connected with their anomalously low viscosity [7]. However, the nature of this phenomenon has not been studied sufficiently, because the collective properties of liquids – in particular, liquid water – have been overlooked [8–11], and the true physical mechanisms of melting have not been analyzed at quantum-mechanical atomic and molecular levels. The collective properties of vibrational modes become strengthened with the growth of cluster-globular water formations in size. As a result, hydrogen bonds also become

© M.E. KORNIENKO, N.L. SHEIKO,
O.M. KORNIENKO, T.YU. NIKOLAIENKO, 2013

ISSN 2071-0194. Ukr. J. Phys. 2013. Vol. 58, No. 2

stronger, which manifests itself in a considerable intensity enhancement for the valence water ν_{OH} bond bands in IR absorption and Raman spectra. Owing to the collectivization of vibrational excitations in liquids, nonlinear resonance interactions between vibrational modes start to play a crucial role; they are accumulated in space and give rise to substantial effects [12–14]. This situation is well-known in laser physics and nonlinear optics, but has not hitherto been taken into account in the physics of quasiliquid films on the surface.

The nonlinear generation of excited vibrational states results in an anomalous enhancement of vibration–electron and intermolecular interactions [15, 16], which is essential for a change of nanoobject properties – in particular, for a decrease of the water freezing temperature and an increase of the water density in nanolayers. Nanomaterials contain a considerable fraction of surface particles with an enhanced anharmonicity of vibrations. Nonlinear wave interactions often play a dominating role at that, in contrast to bulk media, where nonlinear susceptibilities are substantially lower. For instance, with the use of vibrational spectroscopy methods, we earlier found considerable variations in the properties of adsorbed water in disperse and nanoporous silicate media, which are similar to phase transitions [17]. The application of disperse media with a substantial surface area allows a weak signal from separate liquid nanofilms to be considerably amplified for the variation in the properties of water nanolayers to be reliably observed, when their thickness increases, taking advantage of spectroscopy techniques [17].

In this work, a similarity between the properties of the thinnest water layers adsorbed on the surface of fine-dispersed SiO_2 and those of quasiliquid water films on the surface of ice crystallites is used to develop new concepts concerning the formation of quasiliquid nanofilms and their properties in the premelting temperature region. In contrast to the majority of works devoted to studying the plane water nanofilms, we consider the total signals related to the viscoelastic properties of polycrystalline ice in the premelting temperature interval, similarly to what is made for disperse silicate media. This enabled us to research the properties of the thinnest water nanofilms on the ice surface at the initial stages of their formation in a wider temperature interval (from -60 to 20 °C), which creates

large difficulties if separate plane water nanofilms are investigated.

When ice melts, the vibrational instability of the condensed matter state manifests itself [18, 19]. Therefore, if visible [20, 21] or x-ray [22, 23] radiation with the energy of quanta considerably exceeding the instability threshold is applied for studying the properties of water nanolayers on the ice surface, it gives rise to badly controllable strong perturbations in the examined system. In particular, it concerns an anomalously wide spread of obtained results [21]. Instead, the application of a less perturbative method of IR spectroscopy in the overtone range [17] allowed the existence of three discrete quantum states of adsorbed water on the surface of disperse SiO_2 to be established. This discovery is confirmed by a discrete change in the positions of three spectral components belonging to the bands of valence mode overtones $2\nu_{\text{OH}}$ and $3\nu_{\text{OH}}$, which is associated with the increasing thickness of adsorbed water nanofilms [17]. The discrete spectral modifications in the absorption spectrum of adsorbed water can be connected with the formation of discrete nanostructures, i.e. clusters of water molecules. These results allow the problem dealing with the manifestation of discrete properties of water nanofilms on the ice surface to be tackled in a different way.

In this work, we carried out a weakly perturbing experimental research of quasiliquid water films. For this purpose, we analyzed the temperature dependence of the complex shear modulus of polycrystalline ice $G = G_1 + iG_2$ and focused our attention on its imaginary part, the viscous loss modulus G_2 . An enhanced sensitivity of the applied technique is connected with the summation of contributions from plenty of quasiliquid nanofilms on the surfaces of polycrystalline ice grains and an anomalous strong reduction of the $G_{1,2}$ magnitude by 8 or 9 orders of magnitude at the ice-to-water transition. The new ideology and experimental technique allowed the emergence of 5 to 7 discrete nanoformations of quasiliquid water to be registered in the course of growing the nanofilm thickness at the temperature elevation. For the analysis of the physical properties of liquid water nanofilms to be comprehensive, the exposition of original results obtained for their viscoelastic properties is preceded by a consideration and a critical analysis of known literature data [20–25]. It especially concerns data on the manifestations of discrete properties of

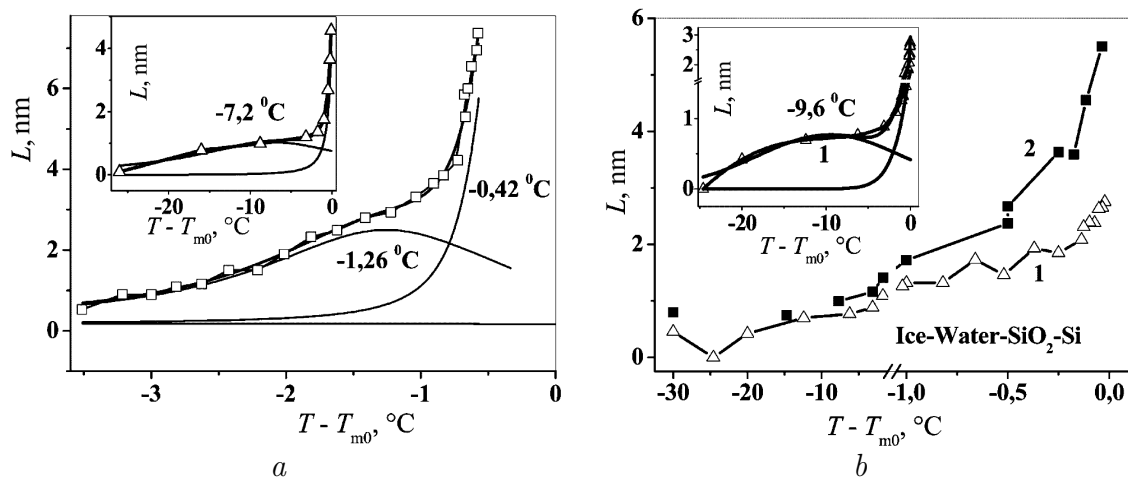


Fig. 1. Temperature dependences of the thicknesses of water nanofilms (a) on the ice surface, which is in contact with air [20] and between ice and SiO_2 surfaces [22] (b and the inset in panel a [21]), as well as their resolution into separate temperature-dependent Lorentzian-like components. In panel b, curve 1 corresponds to a smooth ($d = 15.5 \text{ \AA}$, $\sigma = 2.7 \text{ \AA}$) and curve 2 to a rough ($d = 20.4 \text{ \AA}$, $\sigma = 4.7 \text{ \AA}$) surface of SiO_2 oxide on the (001) and (111) planes, respectively, of silicon crystal

water nanofilms in the temperature dependences of their thickness, $L(T)$. These data are necessary to get a more profound understanding of original results obtained in this work while studying the viscous loss modulus. For the first time, we have analyzed the cluster structure of quasiliquid water nanofilms in the ice premelting region and the connection of this phenomenon with the temperature digitization of melting in nanolayers [25].

2. Discrete Properties of Quasiliquid Nanofilms on the Ice Surface

The dependence $L(\Delta T)$ of the thickness of a single water nanofilm on the surface of ice contacting with water vapor on the temperature difference $\Delta T = T - T_{m0}$, where T_{m0} is the melting temperature of ice, was obtained in works [20, 21] with the use of the optical reflection method and is shown in Fig. 1,a. In Fig. 1,b and in the insets in Figs. 1,a and b, the similar dependences for quasiliquid water nanofilms between the surfaces of ice and SiO_2 layers on the (001) and (111) planes of crystalline silicon are depicted. The results were obtained by reflecting hard x-ray radiation with a wavelength of 0.174 \AA and an energy of about 71 keV [21, 22]. In the cases of clean ice surface and its contact with H_2O vapor, the quasiliquid water nanofilm exists in a temperature interval from about -4 to $0 \text{ }^\circ\text{C}$. In the

absence of water vapor, the interval of existence for a quasiliquid water film gets narrowed to $-1.3 \div 0 \text{ }^\circ\text{C}$ [21]. Quasiliquid water films between ice and SiO_2 surfaces exist in a wider temperature interval from $-30 \text{ }^\circ\text{C}$ (and even lower) to $0 \text{ }^\circ\text{C}$ [22, 23]. This phenomenon can be induced by the rough SiO_2 surface, which is characterized by an enhanced anharmonicity of atomic vibrations and, therefore, promotes the process of surface melting. Alternatively, it can be a result of the application of high-energy x-ray quanta, which increases the vibrational instability of ice in its near-surface regions.

According to the data shown in Fig. 1, the thickness of water nanofilms reaches a value of 4–6 nm and drastically increases in a close vicinity of the phase transition temperature T_{m0} . In particular, according to the optical reflection and ellipsometry data, the thickness of quasiliquid water films can attain 200–1000 nm at $|\Delta T| < 0.1 \div 0.3 \text{ }^\circ\text{C}$ [21]. Generally speaking, we should emphasize considerable variations in the thickness of quasiliquid water layers on the ice surface. For instance, according to the optical reflection data [21] (see Fig. 1,a), the thickness of water nanofilm amounts to $L \approx 2 \text{ nm}$ at $\Delta T = -2 \text{ }^\circ\text{C}$. At the same time, the researches with the use of x-ray radiation scattering at grazing incidence angles give rise to $L \approx 20 \text{ nm}$ [21], whereas the value of L can reach 45 nm at the same temperature according to the data of atomic power microscopy [24]. Hence, providing

identical ΔT -values, the thickness of quasiliquid water layers can change by more than an order of magnitude, which testifies to an extremely high lability of their properties and a substantial influence of high-energy experimental techniques on the results of measurements, which was already mentioned above. A specific sensitivity of the properties of quasiliquid layers on solid surfaces to external factors follows from the resonance nonlinear-wave mechanisms of phase transitions [26, 27]. According to the nonlinear-wave concept of phase transitions, the latent melting heat is connected with the nonlinear generation of higher vibrational modes, which results in the vibrational instability of the substance and a transformation of its electron states. At the same time, nonlinear wave interactions are known to induce extra variations of physical quantities.

The influence of the rough character of SiO_2 nanolayers covering the (001) and (111) planes of Si on the properties of quasiliquid nanofilms can be illustrated on the basis of data exhibited in Fig. 1, *b*. Lower curve 1 of the dependence $L(\Delta T)$ corresponds to a smoother SiO_2 nanolayer with the thickness $d = 1.55$ nm and the characteristic dimension of roughnesses $\sigma = 2.7$ Å [23], which corresponds to the size of H_2O molecule. Upper curve 2 corresponds to a rougher surface of the SiO_2 nanolayer with the average thickness $d = 2.04$ nm and the average roughness $\sigma = 4.7$ Å, i.e. the size close to that of two water molecules. While approaching the temperature $T_{m0} = 0$ °C, the enhanced nonlinearity of the rougher SiO_2 layer brings about an approximately two-fold increase in the thickness of water nanofilms.

All $L(\Delta T)$ dependences in Fig. 1 demonstrate well-pronounced shoulders, which correspond to certain features in the structure of the water nanofilms under study, and even some nonmonotonicities in the dependence $L(\Delta T)$ are observed. In particular, in Fig. 1, *a*, one can see a shoulder at about -1.5 °C, whereas the both insets in Fig. 1 illustrate the existence of the intervals of weak temperature-induced variations of the nanofilm thickness at about -10 °C. In Fig. 1, *b*, one can see that, after a “plateau” $L \approx \text{const}$ in the interval from -20 to -5 °C, where different roughnesses of SiO_2 nanolayers weakly manifest themselves, a “quasiplateau” (weak oscillations of the thickness) is observed in the temperature interval from -1 to -0.25 °C for a smoother SiO_2 layer (curve 1). If the roughness of the SiO_2 nanolayer that contacts with

the water nanofilm is higher, a drastic growth of the water film thickness L is observed in the same temperature interval, which testifies to a possibility for a number of scenarios describing the formation of water nanofilms at the ice premelting and predicting different properties of the formed nanofilms to exist.

The temperature-related features in the formation and the properties of quasiliquid nanofilms on the ice surface can be presented more illustratively by decomposing the dependences $L(\Delta T)$ obtained earlier [20–23] into separate components of a given form. Our numerical analysis showed that the most optimum is the decomposition of the dependence $L(\Delta T)$ into Lorentzian components, which is illustrated in Fig. 1. The dependence in Fig. 1, *a* reveals the existence of two Lorentzians with the maxima at -1.26 and -0.42 °C. The “quasiplateau” in curve 1 in the temperature interval from -1 to -0.25 °C (Fig. 1, *b*), which was discussed above, may probably have the same origin as the feature at about -0.4 °C does (Fig. 1, *a*). In the insets in Fig. 1, one can clearly distinguish sections in a vicinity of -7.2 (panel *a*) and -9.6 °C (panel *b*), where the thickness of water nanofilms varies more smoothly with the temperature. Moreover, after $L \rightarrow 0$ at $T = -24.6$ °C in the dependence $L(\Delta T)$ in Fig. 1, *b* (curve 1), the surface quasiliquid layers are observed at $T = -30$ °C with effective thicknesses of about 0.45 and 0.8 nm, which considerably exceeds the thickness of a single monolayer of water molecules. The observation of such water “nano islands” at lower temperatures and their absence at higher ones can be explained by a nonintegral character of thin water nanofilms and the existence of definite temperature intervals, in which such island films turn out more stable. The procedure applied to the examined dependences $L(\Delta T)$ to decompose them into elementary temperature-dependent components allowed us to find those discrete regions of enhanced stability of water nanofilms at ice premelting.

Our preliminary analysis of some $L(\Delta T)$ dependences known from the literature made it possible to distinguish not less than 3 or 4 temperature intervals with enhanced stability of quasiliquid water nanoformations on the ice surface. In the region of enhanced stability of nanoformations, their thicknesses remain almost invariable within some temperature interval, being substantially thicker than a single monolayer of water molecules. The analyzed data showed that the

minimum thickness of such nanoformations is equal to the thickness of 2 to 3 monolayers of H₂O molecules.

It is essential that the thickness of water nanofilms grows in a step-like manner when the temperature is elevated. For instance, the thickness of water nanofilms grows approximately from 0.75 to 1 nm when the temperature changes from -9.6 to -7.2 °C, which may correspond to the thickness variation from three to four conditional monolayers of water molecules. According to the results of numerical decomposition of $L(\Delta T)$ dependences, the thickness of stable water nanofilms is approximately equal to 2.5 nm in a temperature interval near -1.26 °C. Thus, we may talk about a discrete variation in the thicknesses of water nanofilms on the ice surface, which stems from the dimension discreteness of molecules and molecular nanoformations.

According to the results of quantum chemical calculations, there can exist both stable closed cyclic clusters of water molecules (H₂O)_{*n*} with $n = 3 \div 8$ [28–30] and more massive spatial clusters of water molecules, e.g., in the form of dodecahedra (H₂O)₂₀, combined pentagonal prisms, and more complicated molecular formations [30–33]. It is natural that the quantum-mechanical structure discreteness of quasiliquid nanolayers on the solid surface gives rise to a discrete character of their properties, which is the subject of this work.

3. Temperature Dependence of the Viscous Loss Modulus of Polycrystalline Ice

The imaginary part of the shear modulus $G = G_1 + iG_2$ characterizes viscodissipative properties of the medium (polycrystalline ice). The temperature dependences $G_2(T)$ were studied with the use of the differential method of torsional vibrations, which was proposed and described in works [34, 35] in detail. The advantage of this method consists in that it enables the measurements of the shear modulus to be carried out for the same specimen in the regime of its continuous heating starting from the temperatures $T < T_{m0}$ and to $T \geq T_{m0}$ irrespective of the aggregate state of the substance to be studied, liquid or solid. In terms of the parameters of free damped oscillations of a torsion pendulum, the imaginary part of in detailshear modulus—the loss modulus G_2 —was determined by the formula

$$G_2 = \frac{4lJ}{\pi R^4}(f\alpha - f_0\alpha_0), \quad (1)$$

where f is the frequency, α is the damping coefficient for free torsional oscillations of the pendulum in a cuvette filled with a researched substance, the zero subscripts relate the corresponding quantities to experiments with an empty measuring cuvette, J is the inertia moment of the mobile pendulum part, l is the specimen length, and R is the internal cuvette radius.

The temperature dependence of the imaginary part of the shear modulus, $G_2(T)$, was measured in a temperature interval from -60 to 20 °C with an increment of about 1 °C. In order to increase the reliability of our researches, we carried out ten independent series of measurements for the dependence $G_2(T)$. In order to reduce the relative measurement error, we averaged the results of ten measurements of $G_2(T)$ carried out at every temperature point in the researched interval. The obtained averaged dependence $G_2(T)$ is shown in Fig. 2,*a*. For the sake of comparison, the inset in this panel exhibits the results of measurements for two experimental series demonstrating the maximum difference between each other. One can see that the measurement results are in rather good agreement in the “wings” of $G_2(T)$ dependence curves. Together with rather a small spread of experimental points even in the interval of dependence maxima, this fact characterizes the accuracy of measurements. At the same time, the discrepancies in the region of maxima considerably exceed the measurement accuracy. We associate them with possible extra variations of measured quantities and the bifurcation of modes at nonlinear wave interactions. In turn, this is related to the nonlinear generation of nonequilibrium vibrational states, whose strong excitation gives rise to a vibrational instability in condensed media and a transformation of electron states in the course of melting [18, 19, 26]. The observation of such superregular variations of physical quantities comprises a powerful argument in favor of the nonlinear-wave mechanisms of melting, which will be illustrated in subsequent publications in more details.

In general, the obtained dependence $G_2(T)$ is characterized by a considerable asymmetry with a gradual growth in the low-temperature section and a drastic decrease, when approaching the melting temperature of bulk ice ($T_{m0} = 0$ °C). The maximum of this dependence is located at 262 K (-11 °C) and equal to $G_{2\max} = 315$ MPa. It can be observed below the temperature interval, in which a water nanofilm exists on the free ice surface (from -4 to

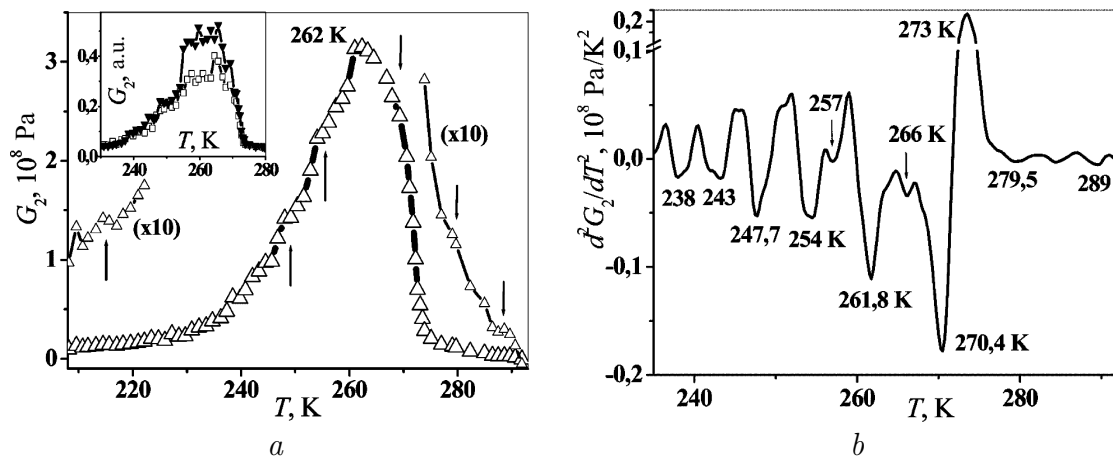


Fig. 2. (a) Temperature dependence of the imaginary part G_2 of the shear modulus averaged over ten independent experiments. The results of two experiments with the largest difference between their results are shown in the inset. (b) Temperature dependence of the second derivative of the experimentally observed dependence $G_2(T)$

0 °C) [21]. Owing to the extremely high sensitivity of the applied technique to premelting processes, we succeeded in registering the variations of the loss modulus G_2 for ice at temperatures lower than 210 K, which is illustrated by a ten-fold scaled-up section in the low-temperature wing of the dependence $G_2(T)$ in Fig. 2,a. For the sake of comparison, the high-temperature wing is also shown scaled up. One can see that the magnitude of G_2 changes by more than seven orders of magnitude on the low-temperature side and by more than eight orders of magnitude in the high-temperature region including the transition into the liquid state. Hence, the applied technique allowed us to discover premelting processes in the temperature range $0.7T_{m0} < T < T_{m0}$.

To compare, the temperature maximum of plasticity in metals at low irradiation doses is observed in the interval $0.35T_{m0} < T < 0.5T_{m0}$ [36]. This fact testifies that the premelting process is a global phenomenon connected with many structural parameters of a substance. The main vibrational and electron states of the latter evolve in a wide temperature interval. This evolution cannot be described in the framework of formal thermodynamic models, without making a detailed analysis of electron and vibrational states, as well as their coupling. This circumstance determines the necessity in a subsequent research of dynamic viscoelastic properties and spectral characteristics of the substance.

In the averaged resulting dependence $G_2(T)$ depicted in Fig. 2,a, one can distinguish the manifesta-

tions of shoulders on the low- and high-temperature sides of the maximum (they are marked by arrows), as well as weak lateral maxima. These peculiarities testify to changes in the structure and properties of quasiliquid layers on the grain surfaces of a polycrystalline ice specimen and can be associated with a discrete variation of the water nanofilm thickness (see Fig. 1). The corresponding features in the structure and properties of water nanofilms on the ice surface can be detected more reliably by analyzing the second derivative of the function $G_2(T)$, which was calculated numerically with the use of averaged experimental data. For the calculation of d^2G_2/dT^2 to be more proper, we carried out a linear interpolation of discrete experimental data; simultaneously, we diminished the step of data discretization and additionally smoothed the data. The obtained temperature dependence of d^2G_2/dT^2 is shown in Fig. 2,b. The numbers shown near the minima of d^2G_2/dT^2 indicate their temperature position in terms of Kelvin degrees. Their reliability and independence of measurement errors are confirmed by a good reproducibility of results in every experimental series (it was additionally checked up).

In the temperature dependence of d^2G_2/dT^2 shown in Fig. 2,b, one can distinctly distinguish a number of minima, which correspond to concave sections in the averaged dependence $G_2(T)$ (Fig. 2,a), i.e. to the examined peculiarities of the loss modulus connected with a discreteness of the thickness and properties of quasiliquid water nanofilms.

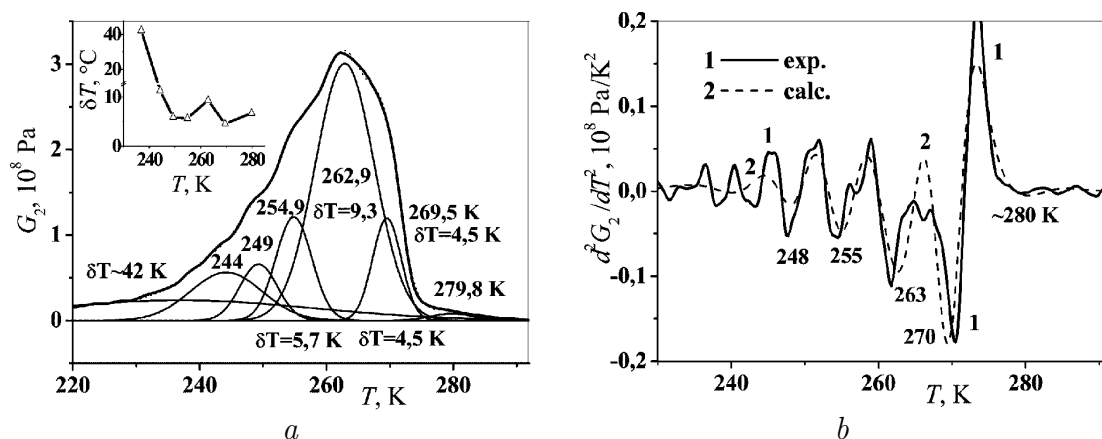


Fig. 3. (a) Results of the numerical decomposition of the resulting experimental dependence $G_2(T)$ into Gaussian-like components. (b) The second derivatives of the experimentally observed (1) and calculated (2) $G_2(T)$ -dependences

It is evident that the main minima of d^2G_2/dT^2 monotonously become deeper at the temperature elevation or when approaching the melting temperature of ice $T_{m0} = 0$ °C. The latter is associated with a sharp peak in d^2G_2/dT^2 and corresponds to a drastic reduction of dG_2/dT at the ice-to-liquid transition. The magnitude of this maximum exceeds the depth of the deepest minimum located in a vicinity of 270 K.

There are a number of peculiarities in the examined temperature dependence of d^2G_2/dT^2 . (i) The maximum of function $G_2(T)$ corresponds to the minimum of its second derivative in a vicinity of 262 K, and the absolute minimum of d^2G_2/dT^2 is reached at a temperature that is higher than the location of the maximum of $G_{2\max}$. (ii) The temperature interval between the minima of d^2G_2/dT^2 increases from 5 to 8 K, as the temperature grows. However, there emerge additional minima at that, which are located between the main ones. For instance, the minimum at 266 K is equidistant with respect to two main peculiarities in vicinities of 262 and 270 K. (iii) Some features are observed in the range of liquid water ($T > 273$ K), which can be associated with the metastability of and spatial inhomogeneities in water. The corresponding amplitudes of d^2G_2/dT^2 variation are much smaller than those of additional minima in vicinities of 257 and 266 K. Nevertheless, they clearly manifest themselves in the form of lateral maxima in the dependence $G_2(T)$ (Fig. 2,a). (iv) Some of the d^2G_2/dT^2 minima reveal themselves in the lower-temperature region (210–235 K) – e.g., near 224, 228, and 232 K –

with a reduced interval between them, which approximately equals 4 K.

In addition, a number of fine peculiarities taking place within the interval of 270–273 K may turn out hidden owing to the smoothing procedure and a drastic variation of the second derivative between the main extremes. The revealed regularities in the behavior of d^2G_2/dT^2 are confirmed, to a great extent, by the differential scanning calorimetry data, which are considered in the next section.

In order to extract the individual contributions of discrete temperature peculiarities to the averaged experimental dependence $G_2(T)$, the latter was numerically decomposed into separate temperature-dependent components of a given form. The number of components in the decomposition was determined with regard for the main minima in the second derivative d^2G_2/dT^2 (Fig. 2,b). In the course of numerical decomposition of the function $G_2(T)$ into separate components, the least-square method was used, in which the temperature position of components, their shapes (Lorentzian or Gaussian), intensities, and halfwidths were varied. It turned out that the averaged experimental dependence $G_2(T)$ can be better represented by a sum of Gaussian-like components.

The obtained results are depicted in Fig. 3,a. The temperatures of the maxima of separate components and the temperature halfwidths δT for some of them are also indicated. The correctness of the decomposition is confirmed by good agreement between the second derivatives d^2G_2/dT^2 from the experimental

and calculated functions $G_2(T)$ (Fig. 3,b). Only one component with a maximum at about 280 K was considered in the liquid-phase interval. One can see that four main minima of d^2G_2/dT^2 near 248, 255, 263, and 200 K, as well as a weaker component at about 280 K in the liquid-phase interval, are reproduced well in the calculated decomposition, which confirms the reliability of marked temperature peculiarities in the structure and properties of water nanofilms on the ice surface.

Since the G_2 -value in the low-temperature wing of the function $G_2(T)$ is approximately 10 times as large as the corresponding values in the high-temperature wing (see Fig. 2.a), the decomposition in Fig. 3,a must inevitably include a wider temperature component. In the examined decomposition, this component has the halfwidth $\delta T \approx 42$ K. It can also reflect the contribution made by several lower-temperature components, e.g., located near 224, 228, and 232 K. The variation of the temperature halfwidth δT with increase in the temperature, which was obtained from the results of numerical decomposition, is shown in the inset in Fig. 3,a. One can see that the magnitude of δT rapidly decreases firstly and, afterward, remains almost constant within the accuracy of calculations. In particular, a somewhat larger halfwidth of the maximum component at 262.9 K stems from the neglect of a probable extra component in a vicinity of 266 K.

Thus, a pronounced sequence of discrete variations in the viscoelastic properties of polycrystalline ice specimens with surface water nanofilms was detected in the wide temperature interval of ice premelting (at 270, 266, 262, 258, 254, 248, 243, and 238 K) and in the interval of liquid phase (at 280 and 288 K).

4. Correlation of the Density Maxima for Water in Nanofilms with the Temperature Intervals of Film Stability

The results of our researches dealing with the discrete structure and properties of water nanofilms on the surface of ice crystallites allow us to revise the results of known measurements of the water density ρ in single plane nanofilms obtained with the use of hard x-ray radiation with a wavelength of 0.174 Å [23]. In those researches, the average density of water in nanofilms, $\rho = (1.19 \div 1.20)$ g/cm³, was determined from the results of ρ -measurements at various temper-

atures and film thicknesses. However, the discovery of discrete features in the temperature dependences of the nanofilm thickness, $L(\Delta T)$, (Fig. 1) and the imaginary part of the shear modulus, $G_2(T)$, which was made while studying the viscoelastic properties of polycrystalline ice in the interval of premelting temperatures, stimulated us to analyze the known temperature series of measurements for the water density ρ in more details. The results obtained for a thinner and less rough SiO₂ layer on the surface of crystalline Si contacting with a water nanofilm are presented in Fig. 4,a. By comparing this figure with both panels of Fig. 1, one can distinctly see that the water density reaches its maximum values of about 1.3 g/cm³ in the regions, where the structure of water nanofilms is stable and their thickness changes weakly with the temperature. Such an almost regular growth of the water density clearly testifies to changes in the water structure.

The results of spectral researches of water nanofilms on the ice surface carried out by us and their detailed comparison with the results of quantum chemical calculations of water clusters (H₂O)_n [28–32], which will be reported in the next work, testify to the formation of closed water clusters on the ice surface. It is pertinent to present two arguments in favor of this statement. (i) The temperature intervals of enhanced stability for the cluster structure of water layers with a collective increase in the hydrogen-bond energy and a definite squeezing of the substance structure [19] are in agreement with the experimentally observed increase of the density in water nanolayers to 1.2–1.3 g/cm³ [23]. (ii) According to the tabulated data [23], the experimentally measured values for the ice surface roughness, $\sigma(T)$, which are shown in Fig. 4,a, are also attained in the regions, where closed water clusters with an increased water density are formed. For a better representation, the results for σ in Fig. 4,a are scaled up by a factor of five. It is meaningful that the maximum values for $\sigma(T)$ are comparable with the size of H₂O molecules. Moreover, $\sigma = 0$ between the intervals of cluster structure stability, and the water density becomes lower.

Those facts comprise additional arguments in favor of the existence of temperature intervals, where the cluster structure of water nanofilms is stable at the ice premelting. At viscoelastic deformations of ice columns, rotations of closed water clusters and changes in the orientation of ice polycrystals are pos-

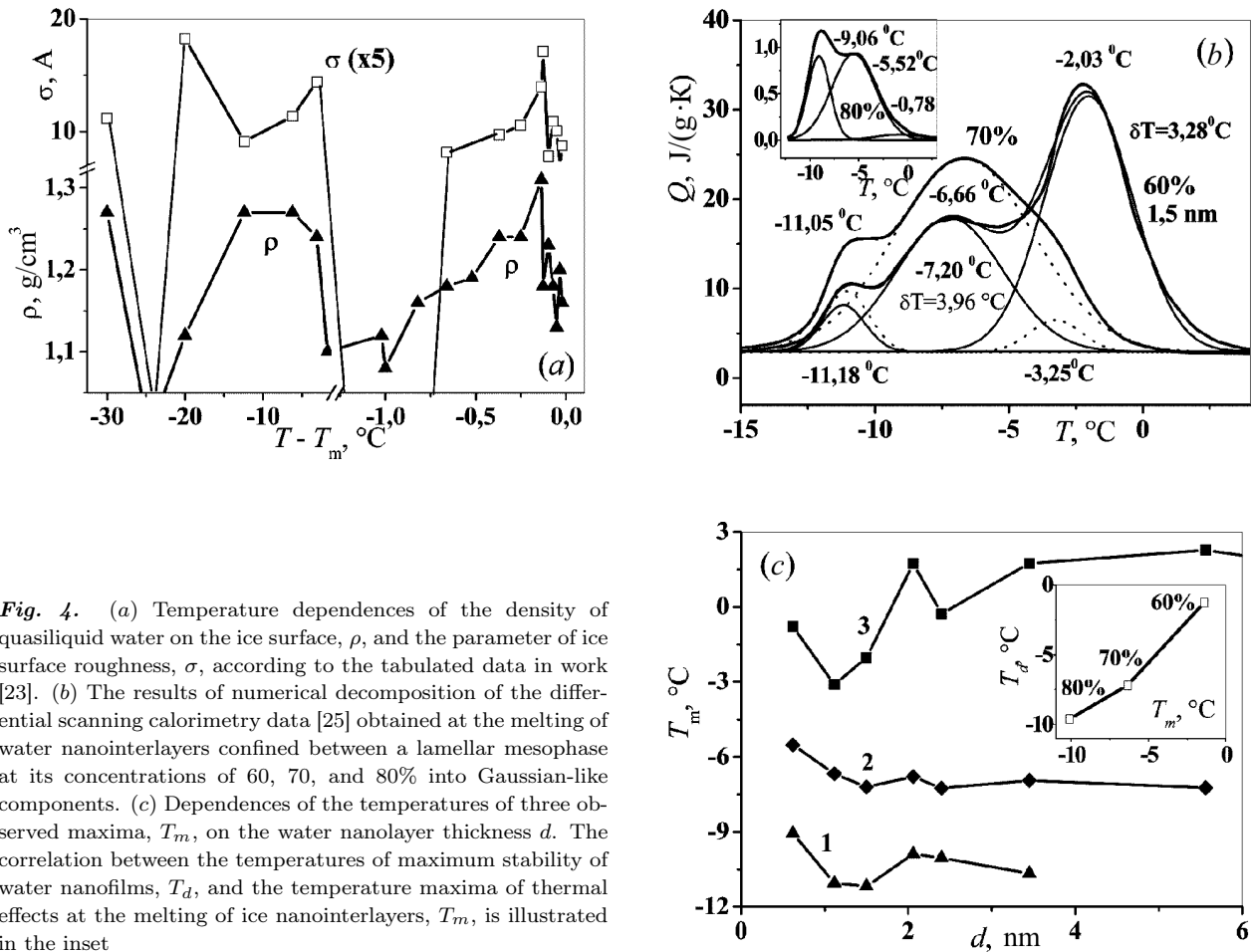


Fig. 4. (a) Temperature dependences of the density of quasiliquid water on the ice surface, ρ , and the parameter of ice surface roughness, σ , according to the tabulated data in work [23]. (b) The results of numerical decomposition of the differential scanning calorimetry data [25] obtained at the melting of water nanointerlayers confined between a lamellar mesophase at its concentrations of 60, 70, and 80% into Gaussian-like components. (c) Dependences of the temperatures of three observed maxima, T_m , on the water nanolayer thickness d . The correlation between the temperatures of maximum stability of water nanofilms, T_d , and the temperature maxima of thermal effects at the melting of ice nanointerlayers, T_m , is illustrated in the inset

sible, which gives rise to a growth of the viscous loss function $G_2(T)$ (the imaginary part of the shear modulus). An additional dispersion of ice stimulated by its deformations is also possible at that. Those processes can be active at lower temperatures, which can explain the emergence of additional closely located minima in the second derivative d^2G_2/dT^2 at $T < 255$ K (see Fig. 2,b).

5. Relation Between the Premelting Phenomena and the Temperature-Heat Discretization at Nanostructure Melting

Similar to thin films of quasiliquid water on the ice surface, water nanolayers of the thickness $d = (1.5 \div 18.6)$ nm can emerge between confining layers of a lamellar mesophase. In work [25], the properties of such water nanolayers were studied using the

method of differential scanning calorimetry (DSC), and three pronounced maxima of thermally induced effects were revealed in the interval from -11 to 2 °C. The thickness of water nanolayers diminished with increase in the mesophase concentration. It is very important that those results concern water nanolayers, the thickness of which is approximately the same as that of quasiliquid water layers on the ice surface. Therefore, those results can be very useful in understanding the ice premelting phenomenon.

We performed a detailed numerical treatment of graphic data presented in work [25]. Some of the results obtained are illustrated in Fig. 4,b. In this figure, the decompositions of DSC temperature data into separate components of a given form at mesophase concentrations of 60, 70, and 80% are depicted. Those are the concentrations, at which the thinnest (less than 1.5 nm) water nanolayers are realized, which

links them with the properties of quasiliquid water films in the ice premelting interval. Our research showed that the best results are obtained if the Gaussian form is used for the decomposition into separate components.

One can see that the positions of maxima for thermal components calculated for the water nanolayer thickness $d \approx 1.5$ nm are in very good agreement with the stability intervals for water nanofilms on the ice surface (see Fig. 1); namely, these are -9.6 , -7.2 , and -1.26 °C. At a water nanolayer thickness of 1.5 nm, the main maximum of heat absorption takes place at a temperature of about -2 °C, which is close to the melting temperature for massive ice specimens ($T_{m0} = 0$ °C). At higher concentrations of the liquid crystal phase (70–80%), more disperse states of water are formed and the maximum of thermal effects shifts to the interval, where the central of three peaks dominates (at about -6.7 °C) (see Fig. 4,b). For a smaller water quantity, the largest maximum of thermal effects is shifted into the low-temperature region ($T \approx -9.1$ °C), as is shown in the inset in Fig. 4,b, although the magnitude of those effects becomes approximately 30 times smaller at that.

The dependences of the temperatures of thermal-effect maxima on the thickness d of water nanolayers confined between the mesophase lamellae are shown in Fig. 4,c. One can see that, in the range where the thicknesses of water layers are small ($d \approx 1.5$ nm), the temperature interval between the maxima of thermal effects, ΔT , approximately equals 4 °C. In the range of larger thicknesses ($d > 2$ nm), we have $\Delta T \approx 4$ °C at low temperatures, and $\Delta T \approx 8$ °C when approaching the melting temperature of the bulk phase, which corresponds well to the discreteness of minima for the second derivative d^2G_2/dT^2 revealed at studying the viscoelastic properties of polycrystalline ice (see Fig. 2,b). The correlation of the temperature positions of thermal-effect maxima, T_m , averaged over the given set of minimum thicknesses of water nanolayers at mesophase contents of 60, 70, and 80%, with the locations T_d of thermal stability ranges for the thicknesses of water nanofilms on the ice surface (see Fig. 1) is illustrated in the inset in Fig. 4,c.

Hence, the maxima of thermal effects are observed in the temperature intervals of maximum stability of water nanofilms on the ice surface. This fact testifies to a profound fundamental interrelation between those phenomena, which needs further researches. An

anomalous stability of the closed clusters of quasiliquid water on the ice surface in certain temperature intervals seems to be associated with the temperature-heat discretization of the melting process in nanolayers, when the total heat of the phase transition is a sum of three separate contributions. It is important that the reductions of the specific melting heat and the phase transformation temperature at a decrease of the water layer thickness, which were revealed by the authors of work [25], are typical of nanoobjects and are related to the enhanced anharmonicity of vibrations for surface or near-surface atoms. For instance, according to the results of work [37], the melting temperature for gold nanoparticles 2 nm in size decreases by 1000 K in comparison with that for massive gold (1340 K).

6. Conclusions

The experimental researches and the detailed analysis of the ice premelting problem, which were done in this work, allow the following conclusions to be drawn.

1. The application of an original technique at studying the viscoelastic properties of polycrystalline ice, which enables the integrated characteristics to be obtained for a considerable number of quasiliquid nanofilms located on the surfaces of separate crystallites, allowed us to reliably observe a variation of the viscous loss function $G_2(T)$ – the imaginary part of the shear modulus – in a wide temperature interval from -60 to 20 °C. Discrete variations of the loss modulus were detected at temperatures of 270, 266, 262, 258, 254, and 248 K.
2. The discrete behavior of the properties of quasiliquid water nanofilms on the ice surface is confirmed by the existence of temperature intervals, in which the thickness $L(T)$ of those films is constant. The dependences $G_2(T)$ and $L(T)$ were resolved into elementary components, for which the temperature positions and halfwidths were determined.
3. The increase of the water density in nanolayers up to 1.3 g/cm³ was found to occur in the intervals of enhanced temperature stability of water nanofilms. The ice roughness also grows in the same intervals [23]. With regard for the known sum-frequency generation spectra from the ice surface–water nanofilm interface [38, 39] and the results of quantum chemical calculations of water clusters $(\text{H}_2\text{O})_n$ [28–33], the crucial role of cluster structure in both water nanofilms and the surface of ice single crystals was demonstrated.

4. A close connection between the discrete dissipative quasiviscous properties and the thicknesses of water nanofilms was established. Three pronounced maxima of thermal effects at the phase transitions in water nanofilms confined between lamellar layers of the mesophase were revealed. All those parameters were found to have peculiarities in the same temperature intervals (from -11 to -10 °C, from -7 to -6 °C, and from -3 to -1 °C), which evidences the common nature of different phenomena. Since the specific heat of bulk ice melting and the limiting value of the sum of integrated heats for three peaks of thermal effects discovered in water nanofilms using the differential scanning calorimetry method [25] are equal to each other, a conclusion can be drawn concerning the ice premelting as an integrated process, in which the vibrational-electron instability of the ice structure is developed.

5. For 5–7 discrete peculiarities, which were detected in the viscoelastic properties of polycrystalline ice at its premelting, a reduction of the temperature distance between them, ΔT , from 8 to 4 °C is observed, as the temperature decreases below -25 °C. This fact correlates with the behavior of the intervals ΔT between the DSC peaks at a change of the water nanofilm thickness in a lamellar structure [25]. This can be a manifestation of the additional deformation instability of the ice structure (similarly to a nanodispersion of metals at the twist extrusion [40] that is widely used in modern materials science).

To summarize, we have established the interrelation of a wide range of phenomena, in particular, between the viscoelastic and thermal properties of nanostructures. The next work will be devoted to spectral methods of studying the discrete properties of water nanofilms in the ice premelting interval. This will allow us to consider the wave and quantum-mechanical manifestations of the premelting phenomenon more comprehensively.

1. V.F. Petrenko and R.W. Whitworth, *Physics of Ice* (Oxford Univ. Press, London, 1999).
2. Yu.I. Golovin, A.A. Shibkov, and O.V. Shishkina, *Fiz. Tverd. Tela* **42**(7), 1250 (2000).
3. T. Bryk and A.D.J. Haymet, *J. Chem.Phys.* **117**, 10258 (2002).
4. I.A. Ryzhkin and V.F. Petrenko, *Zh. Eksp. Teor. Fiz.* **135**, 77 (2009).
5. G.S.Bordonskii and S.D.Krylov, *Pis'ma Zh. Tekhn. Fiz.* **35**, No. 7, 80 (2009).
6. G.S. Bordonskii, A.A. Gurulev, and S.D. Krylov, *Pis'ma Zh. Tekhn. Fiz.* **35**, No. 22, 46 (2009).
7. G.D. Koposov and A.V. Tyagunin, *Pis'ma Zh. Eksp. Teor. Fiz.* **94**, 406 (2011).
8. M.E. Kornienko, *Ukr. Fiz. Zh.* **46**, 546 (2001).
9. M.E. Kornienko, *Ukr. Fiz. Zh.* **47**, 361 (2002).
10. N.E. Kornienko, V.I. Malyi, G.V. Ponezha, and E.A. Ponezha, *Dokl. AN UkrSSR, Ser. A*, No. 4, 65 (1983).
11. N.E. Kornienko, V.I. Malyi, G.V. Ponezha, and E.A. Ponezha, *Opt. Spektrosk.* **60**, 1171 (1986).
12. N.E. Kornienko, *Kvant. Elektron.* **12**, 1595 (1985).
13. M.E. Kornienko, *Ukr. Fiz. Zh.* **47**, 435 (2002).
14. N.E. Kornienko, *Fiz. Zhivogo* **16**, No. 1, 5 (2008).
15. M.E. Kornienko, *Visn. Kyiv. Univ. Ser. Fiz. Mat. Nauky* No. 3, 489 (2006).
16. N.E. Kornienko, N.P. Kulish, S.A. Alekseev, O.P. Dmitrenko, and E.L. Pavlenko, *Opt. Spectrosc.* **109**, 742 (2010).
17. N.E. Kornienko, V.I. Grigoruk, A.N. Kornienko, and S.A. Alexeev, in *Abstracts of the 2nd International Scientific Conference "Nanostructure materials-2010: Belarus-Russia-Ukraine Nano-2010"* (Ukraine, Kiev, 2010), p. 98 (in Russian).
18. N.E. Kornienko, V.I. Grigoruk, and A.N. Kornienko, *Vestn. Tambov. Univ. Ser. Estestv. Tekhn. Nauki* **15**, 953 (2010).
19. N.E. Kornienko, V.I. Grigoruk, and A.N. Kornienko, in *Proceedings of the International Scientific Conference "Challenging Problems in Solid-State Physics", 18-21 October 2011, Minsk* (Minsk, 2011), Vol. 1, p. 26 (in Russian).
20. M. Elbaum and J. S. Wettlaufer, *Phys. Rev. E* **48**, 3180 (1993).
21. J.G. Dash, A.W. Rempel, and J.S. Wettlaufer, *Rev. Mod. Phys.* **78**, 695 (2006).
22. S. Engemann, H. Reichert, H. Dosch, J. Bilgram, V. Honkimaki, and A. Snigirev, *Phys. Rev. Lett.* **92**, 205701 (2004).
23. S.Ch. Engemann, *Ph.D. thesis* (Max-Planck-Institut für Metallforschung, Stuttgart, 2005).
24. A. Doppenschmidt and H.-J. Butt, *Langmuir* **16**, 6709 (2000).
25. E. Prouzet, J.-B. Brubach, and P. Roy, *J. Phys. Chem. B* **114**, 8081 (2010).
26. M.E. Kornienko, *Visn. Kyiv. Univ. Ser. Fiz. Mat. Nauky* No. 4, 466 (2004).
27. M.E. Kornienko, *Visn. Kyiv. Univ. Ser. Fiz. Mat. Nauky* No. 3, 520 (2005).
28. S.S. Xantheas and T.H. Dunning, *J. Chem. Phys.* **99**, 8774 (1993).
29. H. Cybulski and J. Sadlej, *Chem. Phys.* **342**, 163 (2007).

30. M. Losada and S. Leutwyler, *J. Chem. Phys.* **117**, 2003 (2002).
31. H.M. Lee, S.B. Suh, J.Y. Lee, P. Tarakeshwar, and K.S. Kim, *J. Chem. Phys.* **112**, 9759 (2000).
32. G.S. Fanourgakis, E. Apra, W.A. de Jong, and S.S. Xantheas, *J. Chem. Phys.* **122**, 134304 (2005).
33. P. Qian, Li-nan Lu, W. Song, and Zh.-zhi Yang, *Theor. Chem. Acc.* **123**, 487 (2009).
34. L.A. Bulavin, O.Yu. Aktan, Yu.F. Zabashta, T.Yu. Nikolaenko, N.L. Sheiko, *Tech. Phys. Lett.* **36**, Issue 3, 279 (2010).
35. N.L. Sheiko, O.Yu. Aktan, Yu.F. Zabashta, and T.Yu. Nikolayenko, *Ukr. Fiz. Zh.* **55**, 299 (2010).
36. I.M. Neklyudov, A.A. Parkhomenko, I.N. Laptev, V.V. Krasil'nikov, and S.E. Savotchenko, in *Proceedings of the 51st International Conference "Challenging Problems of Strength"* (Kharkov, 2001), p. 3 (in Russian).
37. Ph. Buffat and J.P. Borel, *Phys. Rev. A* **13**, 2287 (1976).
38. X. Wei, P.B. Miranda, and Y.R. Shen, *Phys. Rev. Lett.* **86**, 1554 (2001).
39. X. Wei, P.B. Miranda, Ch. Zhang, and Y.R. Shen, *Phys. Rev. B* **66**, 085401 (2002).
40. Y. Beygelzimer, A. Reshetov, S. Synkov, O. Prokof'eva, and R. Kulagin, *J. Mater. Process. Technol.* **209**, 3650 (2009).

Received 10.05.12.

Translated from Ukrainian by O.I. Voitenko

М.Є. Корнієнко, Н.Л. Шейко,
О.М. Корнієнко, Т.Ю. Ніколаєнко

ДИСКРЕТНІ ВЛАСТИВОСТІ КВАЗІРІДКИХ ПЛІВОК
ВОДИ В ОБЛАСТІ ПЕРЕДПЛАВЛЕННЯ ЛЬОДУ.

1. ТЕМПЕРАТУРНІ ЗАЛЕЖНОСТІ ТОВЩИНИ
НАНОПЛІВОК ВОДИ ТА В'ЯЗКОПРУЖНИХ
ВЛАСТИВОСТЕЙ ПОЛІКРИСТАЛІЧНОГО
ЛЬОДУ

Резюме

Експериментально вивчено особливості температурних залежностей властивостей квазірідких плівок води на поверхні кристалітів льоду при його передплавленні. Досліджено в'язкопружні властивості полікристалічного льоду в інтервалі температур -60 – -20 °С. Виявлено особливості в температурних залежностях товщин нанопрошарків води $L(T)$ і уязної частини модуля зсуву $G_2(T)$ (модуля в'язких втрат). Вперше встановлено існування квазіеквідистантних температурних змін модуля в'язких втрат. Порівняння отриманих результатів з літературними даними щодо температурних залежностей $L(T)$, а також густини води в нанопрошарках і шорсткості поверхні льоду дозволяють пов'язати спостережувані особливості з дискретною кластерною структурою квазірідких наноплівок води. Встановлено існування температурних інтервалів підвищеної стійкості кластерної структури наноплівок води, що проявляється у вигляді екстремумів в'язкопружних характеристик льоду в області передплавлення. Вперше розглядається взаємозв'язок явищ передплавлення і температурної дискретизації процесу плавлення в нанопрошарках льоду.